Differential Patterns of Glucose-Induced Electrical Activity and Intracellular Calcium Responses in Single Mouse and Rat Pancreatic Islets

Célia M. Antunes, António P. Salgado, Luís M. Rosário, and Rosa M. Santos

Although isolated rat islets are widely used to study in vitro insulin secretion and the underlying metabolic and ionic processes, knowledge on the properties of glucose-induced electrical activity (GIEA), a key step in glucose-response coupling, has been gathered almost exclusively from microdissected mouse islets. Using a modified intracellular recording technique, we have now compared the patterns of GIEA in collagenase-isolated rat and mouse islets. Resting membrane potentials of rat and mouse β-cells were approximately –50 and –60 mV, respectively. Both rat and mouse β-cells displayed prompt membrane depolarizations in response to glucose. However, whereas the latter exhibited a bursting pattern consisting of alternating hyperpolarized and depolarized active phases, rat β-cells fired action potentials from a nonoscillating membrane potential at all glucose concentrations (8.4–22.0 mmol/l). This was mirrored by changes in the intracellular Ca^{2+} concentration ($[Ca^{2+}]_i$), which was oscillatory in mouse and nonoscillatory in rat islets. Stimulated rat β-cells were strongly hyperpolarized by diazoxide, an activator of ATP-dependent K^+ channels. Glucose evoked dose-dependent depolarizations and $[Ca^{2+}]_i$ increases in both rat (EC_{50} 5.9–6.9 mmol/l) and mouse islets (EC_{50} 8.3–9.5 mmol/l), although it did not affect the burst plateau potential in the latter case. We conclude that there are important differences between β-cells from both species with respect to early steps in the stimulus-secretion coupling cascade based on the following findings: *1*) mouse β-cells have a larger resting K^+ conductance in 2 mmol/l glucose, *2*) rat β-cells lack the compensatory mechanism responsible for generating membrane potential oscillations and holding the depolarized plateau potential in mouse β-cells, and *3*) the electrical and $[Ca^{2+}]_i$ dose-response curves in rat β-cells are shifted toward lower glucose concentrations. Exploring the molecular basis of these differences may clarify several a priori assumptions on the electrophysiological properties of rat β-cells, which could foster the development of new working models of pancreatic β-cell function. *Diabetes* 49:2028–2038, 2000

From the Center for Neuroscience and Cell Biology (C.M.A., A.P.S., L.M.R., R.M.S.) and the Department of Biochemistry (L.M.R., R.M.S.), Faculty of Sciences and Technology, University of Coimbra, Coimbra, Portugal.

Address correspondence and reprint requests to Rosa M. Santos, Dept. of Biochemistry, FCTUC, P.O. Box 3126, 3001-401 Coimbra, Portugal. E-mail: rmsantos@cnc.cj.uc.pt.

Received for publication 22 February 2000 and accepted in revised form 14 August 2000.

C.M.A. is currently affiliated with the Chemistry Department, University of Evora, Evora, Portugal.

A.P.S. is deceased.

BSA, bovine serum albumin; $[Ca^{2+}]_i$, intracellular Ca^{2+} concentration; GIEA, glucose-induced electrical activity; K_{ATP}, ATP-dependent K^+ channel.

Isolated rat pancreas and islet preparations have been widely used to study in vitro insulin secretion and the underlying metabolic and ionic processes. One of the reasons is that, among small laboratory animals, rats exhibit a biphasic pattern of glucose-induced insulin release very similar to that of humans (1). Yet, another important reason is that the rat pancreas is an abundant source of isolated islets (hundreds of islets can be obtained from a single animal by successful enzymatic digestion), an essential condition for the usefulness of many of the techniques employed in islet studies.

Generation of electrical activity is a key step in glucose-induced insulin release, and it is widely thought to represent the primary mechanism by which Ca^{2+} is imported into the β-cell cytosol, causing an increase in the intracellular Ca^{2+} concentration ($[Ca^{2+}]_i$) and triggering several processes that ultimately result in insulin exocytosis (2). Microelectrode recording of membrane potential from rat islets has been hampered by extreme technical difficulties related to the fact that these islets are small, hard to visualize under the dissecting microscope, and, thus, virtually impossible to isolate in a form amenable to fixation in a conventional electrophysiological chamber. Because these methodological constraints do not apply to mouse islets, intracellular recording of membrane potential has been traditionally carried out using microdissected mouse islets. Islet researchers have therefore been compelled to rely on the latter recordings for studies involving rat preparations. The validity of this extrapolation can, however, be brought into question by growing evidence that both confirmed the original observation (3) that rat and mouse islets exhibit differences in the pattern of glucose-induced insulin release and suggested the existence of clear differences in the pathways underlying stimulus-response coupling. For example, rat islets exhibit an enhanced production of (and sensitivity to) intracellular cAMP when stimulated with glucose (4). Also, glucose stimulation of rat islets induces a five- to sixfold increase in phosphoinositide hydrolysis, in sharp contrast to mouse islets in which virtually no increase was observed (5). Moreover, in rat β-cells, short-term exposure to high glucose induces a potentiation (priming) of the response to subsequent stimulation (6); this phenomenon is absent in mouse β-cells (7).

In a rather preliminary report (8), β-cells from collagenase-isolated cultured rat islets have been claimed to display 7-mV depolarizations in response to 11 mmol/l glucose and concomitant membrane potential fluctuations lasting ~1 s. At this sugar concentration, β-cells from microdissected mouse

islets exhibit slow variations in membrane potential underlying bursts of action potentials, with typical durations and frequencies of several seconds and 1–6 min^{-1}, respectively (9). We have now made a systematic effort to not only characterize glucose-induced electrical activity in collagenase-isolated rat islets, but to actually compare its pattern with that determined from parallel experiments on isolated mouse islets carried out under identical experimental conditions. This was achieved by further developing the recording technique, as described by Ikeuchi et al. (8), that was based on the use of suction glass pipettes to hold in place collagenase-isolated islets. Because previous studies had demonstrated a tight correlation between oscillatory electrical activity and $[Ca^{2+}]_i$ changes (10), we have also compared rat and mouse islets from the standpoint of its cytosolic Ca^{2+} responses to glucose stimulation.

RESEARCH DESIGN AND METHODS

Islet preparation and culture. Female albino mice (Charles River) 3- to 6-months-old and weighing 30–40 g and 9- to 13-week-old female Wistar rats weighing 200–300 g were killed by a blow to the head, followed by cervical dislodgement. Both mouse and rat islets were isolated by collagenase (type P; Boehringer Mannheim) digestion of the pancreas, in accord with established procedures (11,12). Isolated islets were visualized under a stereo microscope and selected by its characteristic round shape, smooth edges, and white color.

In some experiments, islets (henceforth designated as freshly isolated islets) were used shortly (i.e. a few hours) after isolation. These islets were typically incubated in either 11 mmol/l glucose (mouse) or 8.4 mmol/l glucose (rat) for 2 h and were further incubated for at least 50 min in 2 mmol/l glucose before the experiments. The physiological salt solution had the following composition (mmol/l): 120 NaCl, 5 KCl, 25 $NaHCO_3$, 2.56 $CaCl_2$,1.13 $MgCl_2$, and 3% bovine serum albumin (BSA) (pH 7.4 after equilibration with 5% CO_2/95% O_2 in an humidified air atmosphere at 37°C). In other experiments, islets (henceforth designated as cultured islets) were kept in culture for 18–24 h in an RPMI-1640–based medium supplemented with 10% fetal calf serum, antibiotics (100 U/ml penicillin and 100 µg/ml streptomycin), and glucose (11 and 8.4 mmol/l for mouse and rat islets, respectively), pH 7.4. Other tissue culture details have been described by Salgado et al. (12). Like the freshly isolated islets, these islets were further incubated for at least 50 min in 2 mmol/l glucose before the experiments.

Electrophysiological experiments. The membrane potential was recorded from collagenase-isolated islets using a high-impedance amplifier as previously reported (13). Islets were then transferred to a fast perifusion chamber (vol 40 µl), in which they were held in place with the help of a suction pipette. This procedure consisted of a fire-polished glass pipette filled with a physiological salt solution and joined to a fine plastic tubing to which a gentle negative pressure was applied with the help of a syringe. The suction pipette was positioned with a micromanipulator. The perifusion solution was the same as the above physiological salt solution, except that it contained no BSA, was supplemented with different concentrations of glucose as required, and was constantly gassed with 95% O_2/5% CO_2 for a final pH of 7.4. This solution was delivered to the chamber at ~1.5 ml/min (37°C). Solution changes were made with the help of a stop-cock valve. The time required for complete solution exchange at the chamber level was ~8 s (not corrected for in the figures). Islet β-cells were impaled with high-resistance (100–200 MΩ) glass microelectrodes. Input resistance to the β-cell membrane was assessed by injecting rectangular pulses of current (0.1 nA) through the recording microelectrode after null-bridge offset compensation in extracellular solution of the voltage deflexions due to microelectrode resistance, as reported (14). Other electrophysiological details have been described by Rosário et al. (13). Impalement of β-cells was identified by the characteristic cell depolarization in response to 11 mmol/l glucose or tolbutamide.

Microfluorometry. The $[Ca^{2+}]_i$ was measured from single islets using the fluorescent Ca^{2+} indicator fura-2 as described previously (11,12). Briefly, islets were incubated with a physiological salt solution supplemented with 3% BSA, 2 mmol/l glucose and 3 µmol/l fura 2-AM for 45 min at 37°C. The loaded islets were then transferred to a perifusion chamber (30 µl vol, 1.5 ml/min flow rate), placed on the stage of an inverted fluorescence microscope, and allowed to attach to a poly-L-lysine–coated coverslip (used as a chamber bottom) for 10–15 min before starting the experiments. Solution changes were made with a stop-cock, and there was a delay to the chamber of 11 s (not compensated for in the figures). The $[Ca^{2+}]_i$ was measured using a dual excitation microfluorescence system (Deltascan; Photon Technology International, Princeton, NJ). Fura-2 was excited at 340/380 nm, and the fluorescence was detected using an interference filter centered at 510 nm. The data were corrected for background fluorescence and were acquired at 10 Hz by a computer. The fluorescence ratio F_{340}:F_{380} was converted into $[Ca^{2+}]_i$ values using the calibration equation of Grynkiewicz et al. (15), as described previously (11).

Data analysis. All results were expressed as means ± SE. Statistical assessment of differences between mean values was performed using unpaired Student's *t* test.

RESULTS

Figure 1 depicts representative examples of electrophysiological experiments in which freshly isolated rat and mouse islets (islets 1 and 2 in Fig. 1*A* and islet 1 in Fig. 1*B*) were initially exposed to a subthreshold glucose concentration (2 mmol/l) and subsequently challenged with 11 mmol/l glucose. We have also recorded membrane potential from islets (e.g., islet 3 in Fig.1*A* and islet 2 in Fig.1*B*) that have been maintained in culture for 18–24 h to allow full recovery from the isolation procedure.

Resting membrane potential and $[Ca^{2+}]_i$. Rat islet β-cells exhibited a more positive resting membrane potential than mouse islets. Indeed, as shown in Fig. 1*C*, the average membrane potential recorded from freshly isolated rat and mouse islets in 2 mmol/l glucose was –50 ± 2 and –60 ± 3 mV, respectively (n = 8–13 islets, $P < 0.05$). This difference is unlikely to be a consequence of the isolation procedure, because cultured rat islets were also more depolarized than cultured mouse islets in 2 mmol/l glucose (average resting membrane potential –52 ± 3 and –59 ± 2 mV, respectively; n = 8–10 islets; $P < 0.05$). The fact that rat β-cells are relatively more depolarized is consistent with the display of higher levels of noise (flickering potential) by membrane potential recordings in these cells compared with mouse β-cells (Fig. 1). At this point, it should be noted that exposing rat β-cells to diazoxide, an activator of ATP-dependent K^+ (K_{ATP}) channels (16), brought the membrane potential to levels significantly more negative (approximately –20 mV) than those recorded in 2 mmol/l glucose alone (Fig. 2*A*).

We have recorded the $[Ca^{2+}]_i$ from whole collagenase-isolated islets using the fluorescent Ca^{2+} indicator fura-2 (Fig. 4). As shown in Fig. 4*C*, there was no significant difference between resting $[Ca^{2+}]_i$ in rat and mouse islets (67 ± 4 and 55 ± 8 nmol/l, respectively, for freshly isolated islets, n = 8–18; 61 ± 4 and 62 ± 6 nmol/l, respectively, for cultured islets, n = 7–18; $P > 0.05$ in both cases).

Effects of 11 mmol/l glucose on membrane potential and $[Ca^{2+}]_i$. Fig.1*B* shows that glucose (11 mmol/l) depolarized the β-cell membrane and triggered a bursting electrical activity (slow membrane potential waves with action potentials firing from a plateau potential of approximately –35 mV) in collagenase-isolated mouse islets. This phenomenon resembles the typical bursting electrical activity recorded from microdissected mouse islets (17).

Raising the glucose concentration from 2 to 11 mmol/l evoked a prompt membrane depolarization in all rat islets tested (Fig. 1*A*). This finding, however, differed markedly from the glucose response displayed by mouse islets, since there were no oscillations in membrane potential associated with bursting electrical activity. The amplitude of the glucose-induced depolarization was variable from islet to islet and, for the most part, appeared to increase along the first few minutes of stimulation. For freshly isolated islets, the

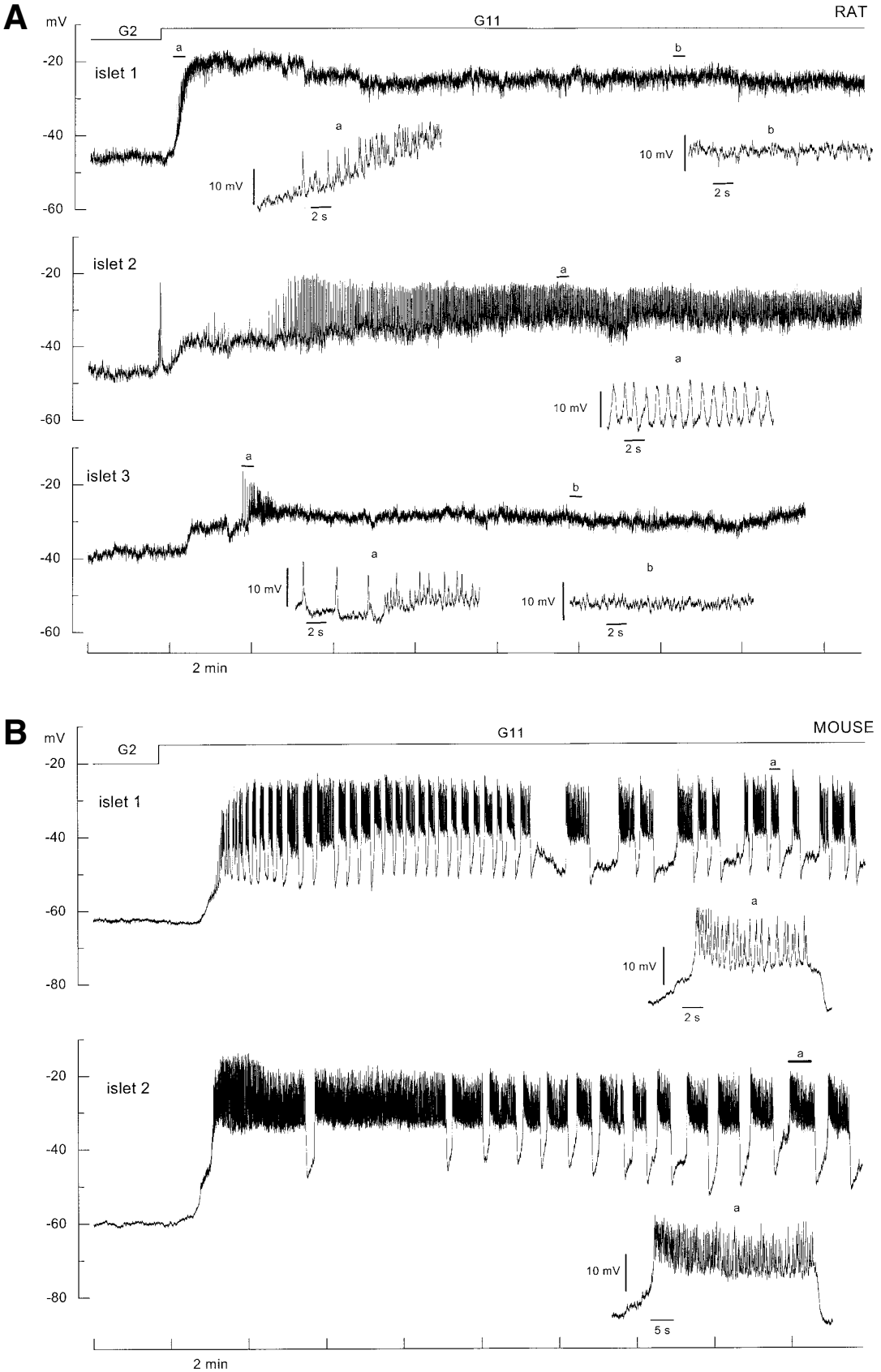

FIG. 1*A* and *B*. Glucose-induced electrical activity in rat and mouse β-cells. Glucose concentration in the perfusion medium was raised from 2 (G2) to 11 mmol/l (G11) as indicated by the horizontal bars. *A*: Typical intracellular recordings from freshly isolated (islets 1 and 2) and cultured (islet 3) rat islets. *B*: Typical intracellular recordings from freshly isolated (islet 1) and cultured (islet 2) mouse islets. Details of electrical activity are shown beneath the main records on an expanded time scale. Islets were isolated by collagenase digestion in all cases. The membrane potential of stimulated β-cells was measured at the foot of the spikes.

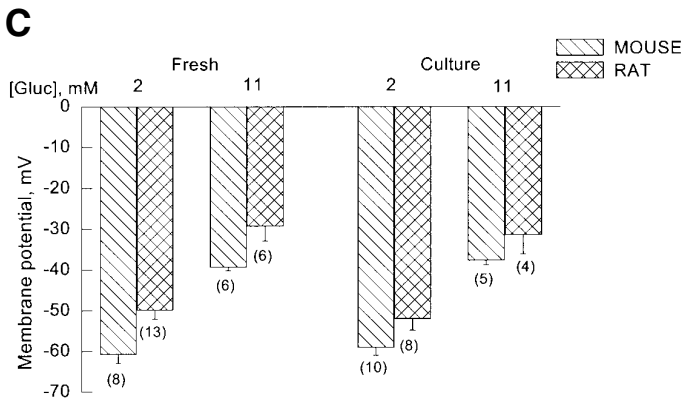

FIG. 1*C*. Average membrane potential responses to glucose stimulation in rat and mouse islets. Data were pooled from the experiments depicted in *A* and *B* and similar experiments. Islets were either used fresh after collagenase isolation (Fresh) or were kept in culture for 18–24 h (Culture), as explained in RESEARCH DESIGN AND METHODS. Measurements were either made in 2 mmol/l glucose or at the steady state in 11 mmol/l glucose, as indicated above the columns. Data are presented as means ± SE (the number of experiments performed is given next to each column in parenthesis).

maximal amplitude of depolarization, defined as the difference between membrane potential at the steady state in 11 mmol/l glucose (foot of the spikes) and resting membrane potential in 2 mmol/l glucose, averaged 23 ± 5 mV (n = 6 islets). This is of the same order of magnitude as the maximal amplitude of depolarization reached in mouse islets (difference between plateau potential and resting membrane potential in 2 mmol/l glucose: 18 ± 2 mV, n = 6 islets) (Fig. 1*C*).

Membrane depolarization was accompanied by the appearance of action potentials in all rat islets examined. However, the amplitude of these spikes was clearly variable from islet to islet (and often within a particular islet), depending on the membrane potential at the foot of the spikes. This is especially evident in islet 1 (Fig. 1*A*, expanded trace *a*), in which well-defined voltage fluctuations (i.e., clearly in excess of basal noise levels) could be observed only over a relatively narrow membrane potential range (approximately –40 to –25 mV). For other islets, the depolarizing effect of glucose was slower and less intense (membrane potentials at the foot of the spikes were more negative than –30 mV at all times), and vigorous spiking persisted throughout an extended interval, albeit with a tendency to decrease in amplitude as the membrane depolarized (e.g., islet 2 in Fig.1*A*). Figure 3*A* (left histogram) relates spike amplitude to membrane potential at the foot of the spikes (data collected from five experiments in which rat islets were stimulated with 11 mmol/l glucose). This analysis shows that spike amplitude increased with membrane potential in the range –50 to –35 mV; spike amplitude decreased for larger depolarizations and became close to basal noise levels for membrane potential values more positive than –25 mV. For mouse islets, the average spike amplitude in 11 mmol/l glucose showed a tendency to decrease with membrane potential in the range

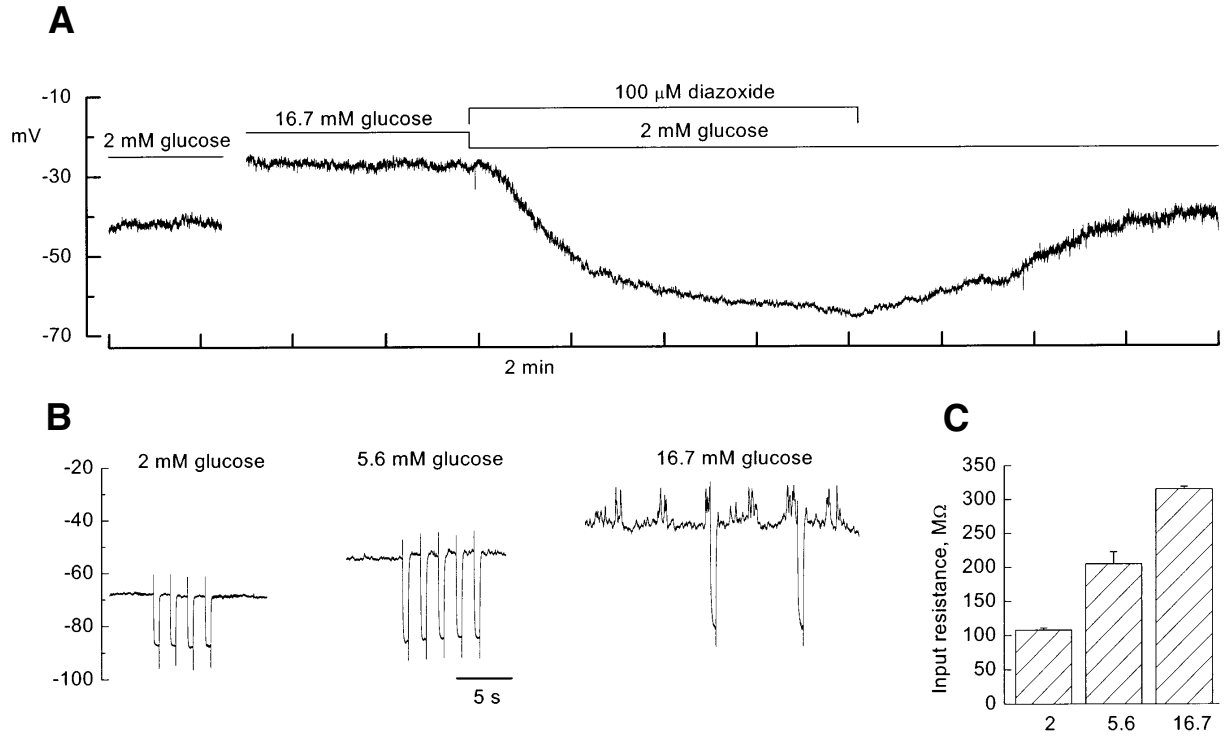

FIG. 2. Effect of glucose and diazoxide on membrane potential and input resistance to the rat β-cell membrane. *A*: Effect of diazoxide. Glucose concentration in the perfusion medium was raised from 2 to 16.7 mmol/l as indicated by the horizontal bars (time in 16.7 mmol/l glucose before record: 12 min). Glucose concentration was then reduced to 2 mmol/l and 100 μmol/l diazoxide applied, as shown. Diazoxide was finally withdrawn in the continued presence of 2 mmol/l glucose. The diazoxide removal resulted in pronounced depolarization of the β-cell membrane. *B*: Voltage deflexions elicited by intracellular current injection. Trains of hyperpolarizing current pulses (0.1 nA) were applied to a β-cell at the steady state of different glucose concentrations (2, 5.6, and 16.7 mmol/l). *C*: Effect of increasing glucose concentration on β-cell input resistance. Input resistance was estimated from the voltage deflexions elicited by intracellular current injection (0.1 nA). Data from the experiment depicted in *B* and two similar experiments. Data are presented as means ± SE.

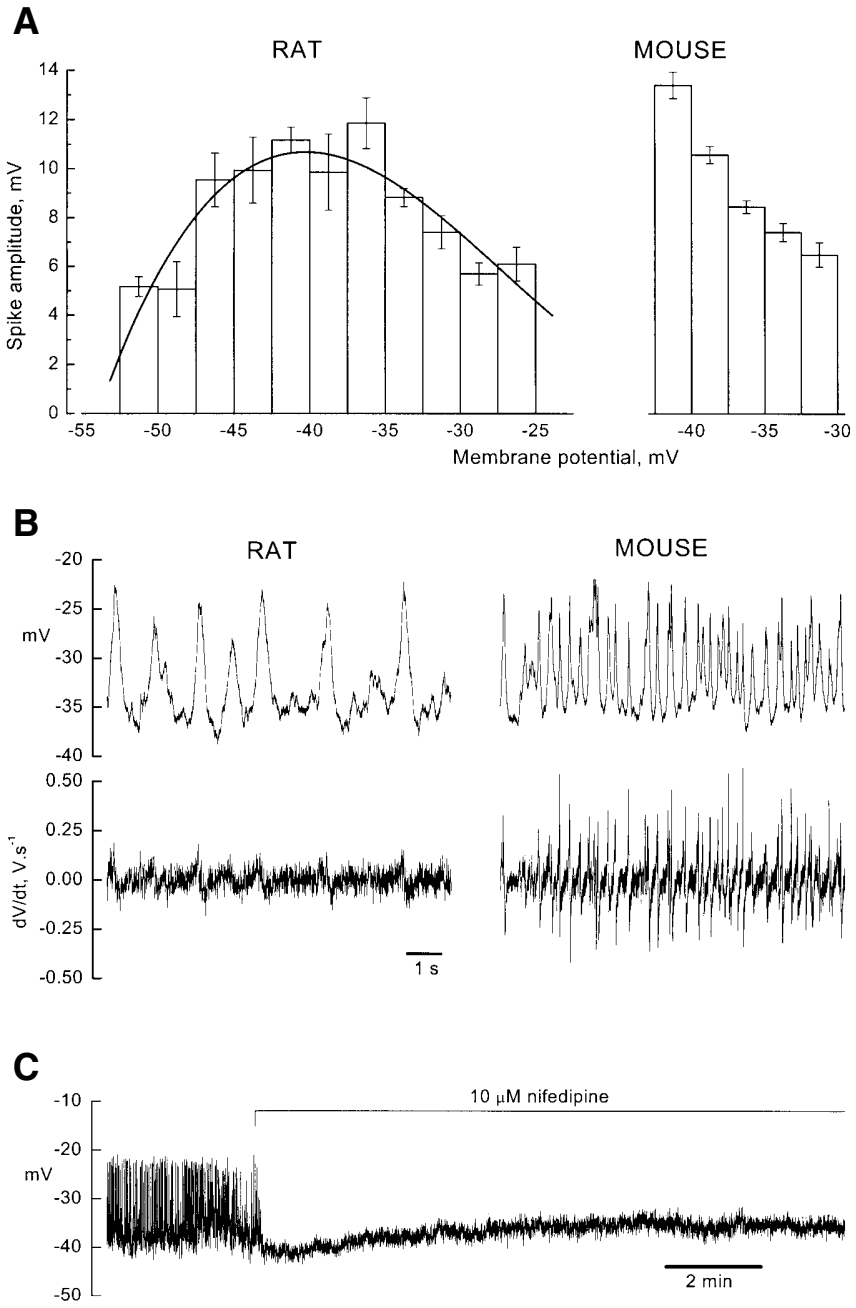

FIG. 3. Characteristics of the action potentials in rat and mouse islets. *A*: Islets were stimulated with 11 mmol/l glucose as in the experiments depicted in Fig. 1. Action potential amplitude was sampled at different times and pooled according to membrane potential at the foot of the spikes. Data are presented as means ± SE (n = 6–23 spikes per 2.5-mV bin from five experiments). *B*: Expanded traces depicting electrical activity in 11 mmol/l glucose and respective first derivatives (dV/dt, bottom panel). *C*: Effect of nifedipine on the electrical activity induced by 5.6 mmol/l glucose in rat islets. The experiment is representative of four similar experiments on rat islets.

–42.5 to –30 mV and was of the same order of magnitude as that measured from rat islets (Fig. 3*A*, right histogram).

We have calculated maximum depolarization and repolarization rates of rat and mouse β-cell action potentials by determining the time derivatives of the membrane potential from expanded traces in 11 mmol/l glucose (range of membrane potential values at the foot of the spikes –35 to –33 mV). Figure 3*B* shows that maximum spike depolarization and repolarization rates were smaller for rat β-cells (average maximum depolarization rates pooled from three similar experiments on rat and mouse islets 0.35 ± 0.02 and 0.67 ± 0.05 V/s, respectively; average maximum repolarization rates –0.24 ± 0.01 and –0.49 ± 0.04 V/s, respectively). The spike depolarization rate in rat β-cells is much lower than would be expected for Na^+ action potentials (or action potentials with a mixed contribution of Na^+ and Ca^{2+} channels) (18), suggesting that it is mainly mediated by the activation of voltage-sensitive Ca^{2+} channels. Accordingly, Fig. 3*C* shows that the L-type Ca^{2+} channel blocker nifedipine abolished the rat β-cell electrical activity induced by 5.6 mmol/l glucose.

We have investigated the effect of 11 mmol/l glucose on $[Ca^{2+}]_i$, as determined from whole mouse and rat islets. Glucose induced a multiphasic $[Ca^{2+}]_i$ response from mouse islets (Fig.4*B*): the $[Ca^{2+}]_i$ transiently decreased to levels below baseline, increased sharply to a peak, and oscillated from an elevated plateau for the remainder of the stimulation. These $[Ca^{2+}]_i$ oscillations originate from oscillatory Ca^{2+} influx associated with bursting electrical activity (10). As shown in Fig. 4*A*, the initial effect of glucose on rat islets was to lower the $[Ca^{2+}]_i$; subsequently, the $[Ca^{2+}]_i$ increased to a peak and either maintained elevation at near peak levels or decreased slowly to a plateau. High-frequency $[Ca^{2+}]_i$ fluctu-

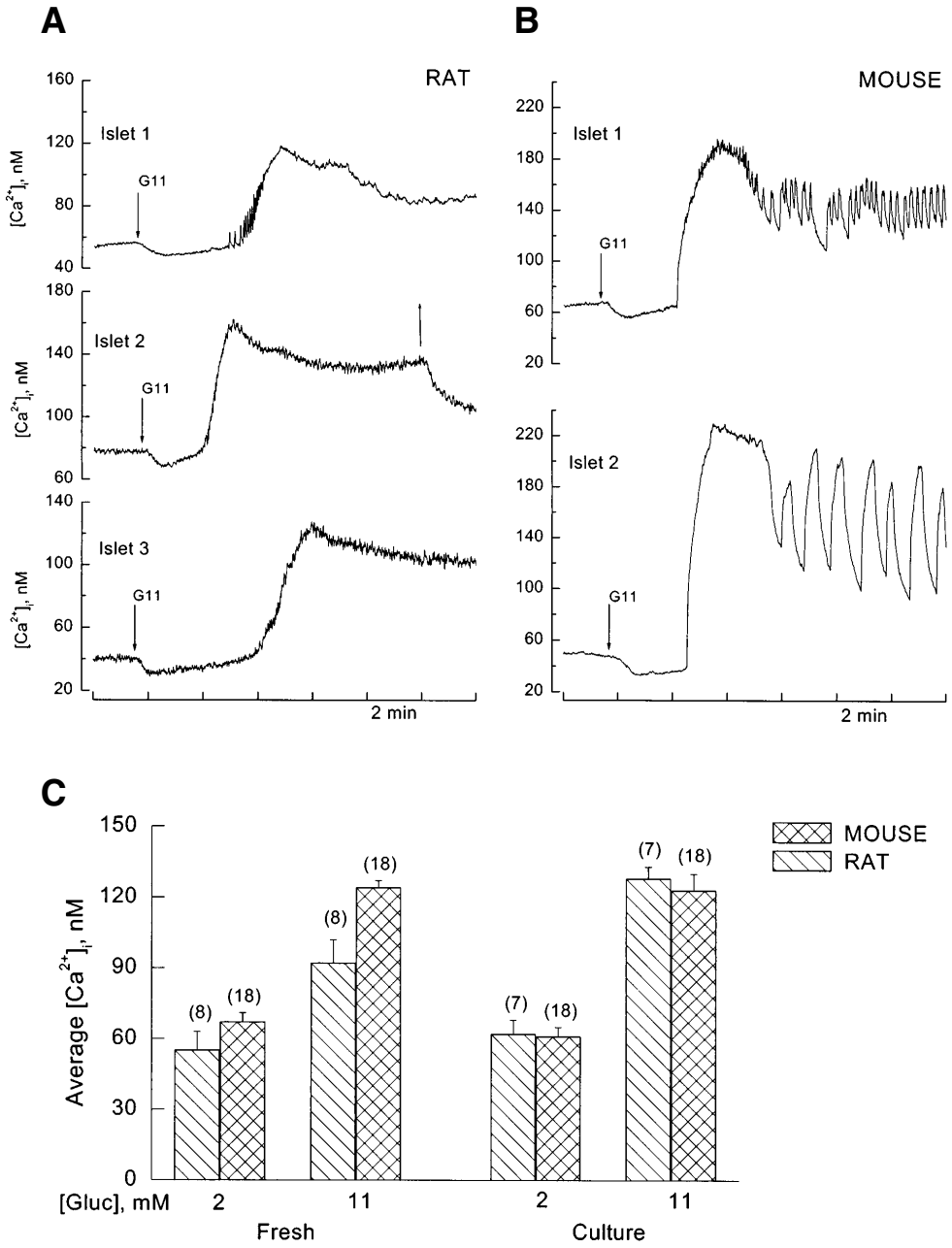

FIG. 4. Effect of 11 mmol/l glucose on $[Ca^{2+}]_i$ in rat and mouse islets. Glucose concentration was changed between 2 and 11 mmol/l (G11) as indicated by the arrows. The vertical scale represents the $[Ca^{2+}]_i$, as measured from whole islets by a dual excitation epifluorescence procedure (RESEARCH DESIGN AND METHODS). *A*: Typical $[Ca^{2+}]_i$ recordings from freshly isolated (islets 1 and 2) and cultured (islet 3) rat islets. *B*: Typical $[Ca^{2+}]_i$ recordings from freshly isolated (islet 1) and cultured (islet 2) mouse islets. *C*: Average $[Ca^{2+}]_i$ responses to glucose stimulation in rat and mouse islets. Data were pooled from the experiments depicted in *A* and *B* and similar experiments. Islets were either used fresh after collagenase isolation (Fresh) or kept in culture for 18–24 h (Culture), as explained in RESEARCH DESIGN AND METHODS. Measurements were made either in 2 mmol/l glucose or at the steady state in 11 mmol/l glucose, as indicated below the columns. The plotted values represent the average $[Ca^{2+}]_i$ at 15–18 min during stimulation. Data are presented as means ± SE (the number of experiments performed is given above each column in parentheses).

ations, reminiscent of the spiking activity displayed by some rat islets, were sporadically recorded at the beginning of the $[Ca^{2+}]_i$ rise (Fig. 4*A*, islet 1; representative of 7 of 22 experiments). Interestingly, peak $[Ca^{2+}]_i$ values were reached between 4 and 6 min of stimulation, regardless of the animal species (286 ± 17 and 338 ± 22 s for mouse and rat islets, respectively; n = 11–22 islets). This matches the time course of the first phase of glucose-induced insulin release (19).

There were some differences between freshly isolated and cultured mouse islets with respect to their responsiveness to 11 mmol/l glucose. For example, while cultured islets displayed a typical biphasic response consisting of continuous spiking followed by regular bursting (Fig.1*B*, islet 2; representative of six islets), most of the freshly isolated islets examined (three of four) exhibited instead an initial pattern of higher frequency bursting (Fig.1*B*, islet 1). It is also noteworthy that the amplitude of

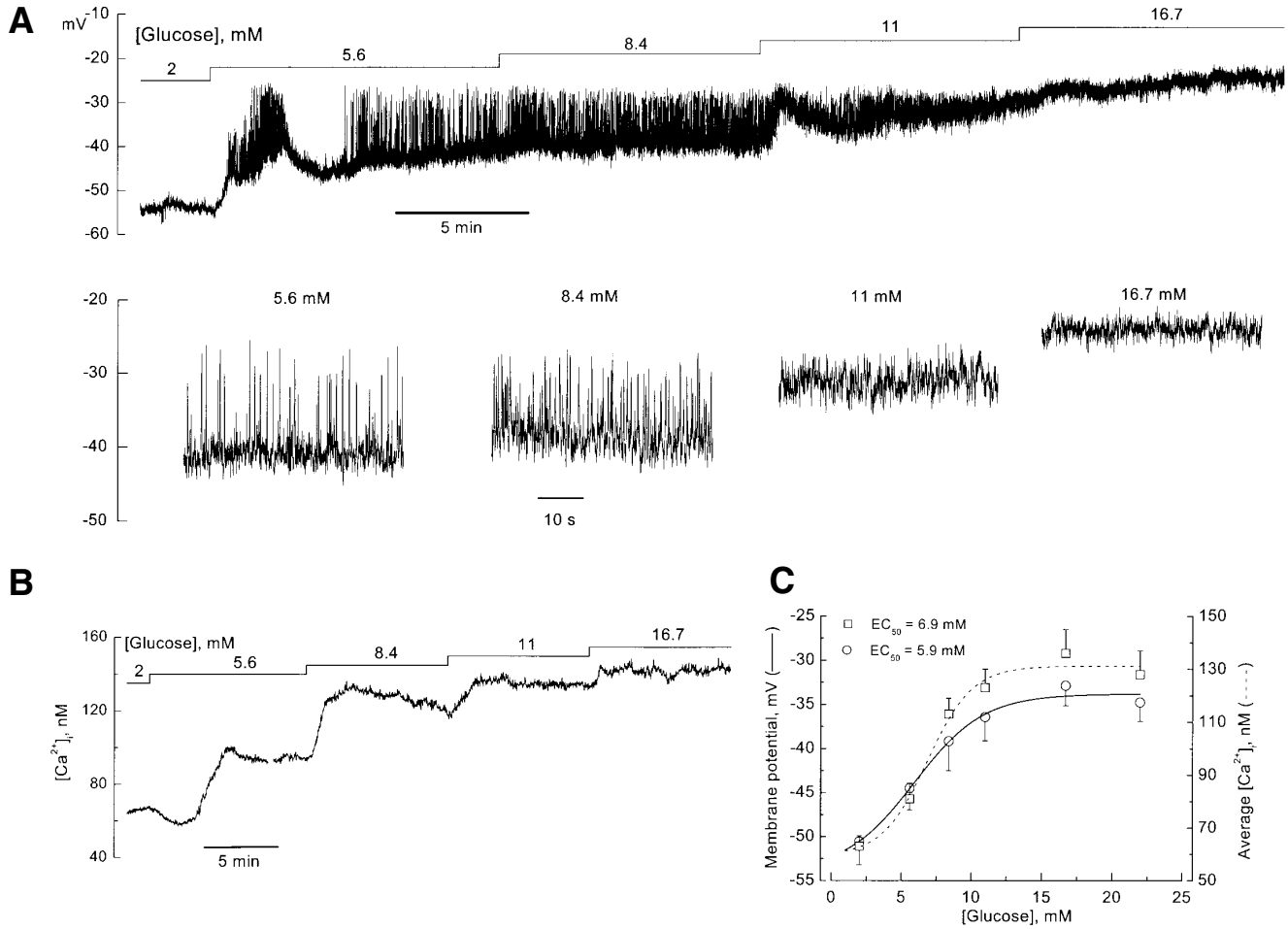

FIG. 5. Dose-dependent effects of glucose stimulation on membrane potential and $[Ca^{2+}]_i$ in rat islets. Islets were stimulated with increasing glucose concentrations as indicated by the horizontal bars. *A*: Effect on membrane potential (freshly isolated islet). Sample records at each glucose concentration (last 50 s) are shown beneath the main trace on an expanded time scale. *B*: Effect on $[Ca^{2+}]_i$ (freshly isolated islet). *C*: Effect of increasing glucose concentrations on membrane potential (foot of the spikes) and $[Ca^{2+}]_i$, measured at the steady state for each concentration (last 120 s). Data were pooled from the experiments depicted in *A* and *B* and other similar experiments using both freshly isolated and cultured islets (n = 7 and 13 islets for the membrane potential and $[Ca^{2+}]_i$ experiments, respectively). Vertical bars represent mean values ± SE.

$[Ca^{2+}]_i$ oscillations is higher in cultured compared to freshly isolated islets (Fig.4*B*; islets 2 and 1, respectively). As a result, the average amplitude of the $[Ca^{2+}]_i$ response, assessed by averaging out the $[Ca^{2+}]_i$ at the steady state, was notably higher for cultured islets (Fig.4*C*). However, as shown in Fig.1*C*, maximal amplitude of depolarization reached in cultured islets did not differ from that in freshly isolated islets.

Freshly isolated and cultured rat islets displayed a similar responsiveness to 11 mmol/l glucose, as shown in Figs. 1*C* and 4*C*. For example, maximal amplitude of depolarization recorded from cultured islets averaged 22 ± 6 mV (n = 4 islets; not significantly different from freshly isolated islets [P > 0.05]). The amplitude of the $[Ca^{2+}]_i$ response in freshly isolated rat islets (55 ± 3 nmol/l, n = 18 islets) was also similar to that recorded from cultured islets (62 ± 4 nmol/l, n = 18 islets) (as shown in Fig.4*A*, in which islets 1 and 2 and islet 3 are examples of freshly isolated and cultured islets, respectively).

Dose-dependent effect of glucose on membrane potential and $[Ca^{2+}]_i$. Rat islets have a lower threshold for glucose-induced insulin release (20,21). It is therefore conceivable that both the membrane potential and the $[Ca^{2+}]_i$ responses might be near maximal at 11 mmol/l glucose, thus accounting for the lack of sustained oscillations at the steady state for this glucose concentration. We have assessed this possibility by continuously recording the membrane potential and $[Ca^{2+}]_i$ in response to stepwise increases in glucose concentration.

Figure 5*A* depicts a typical membrane potential recording from a rat islet stimulated with increasing glucose concentrations in the range 2–16.7 mmol/l. Raising the sugar concentration from 2 to 5.6 mmol/l evoked a multiphasic response, characterized by an early membrane depolarization and concomitant surge of spikes, followed by a slight hyperpolarization without spiking activity; a few minutes later, the cell depolarized to a level 10 mV above resting membrane potential, and spiking activity resumed. Further raising the glucose concentration to 8.4, 11, and 16.7 mmol/l evoked progressive and slow membrane depolarizations, bringing membrane potential at the foot of the spikes to different levels in the range –40 to –25 mV; as a consequence, spike amplitude decreased progressively and became residual at the highest glucose concentration tested. An increase in spike frequency

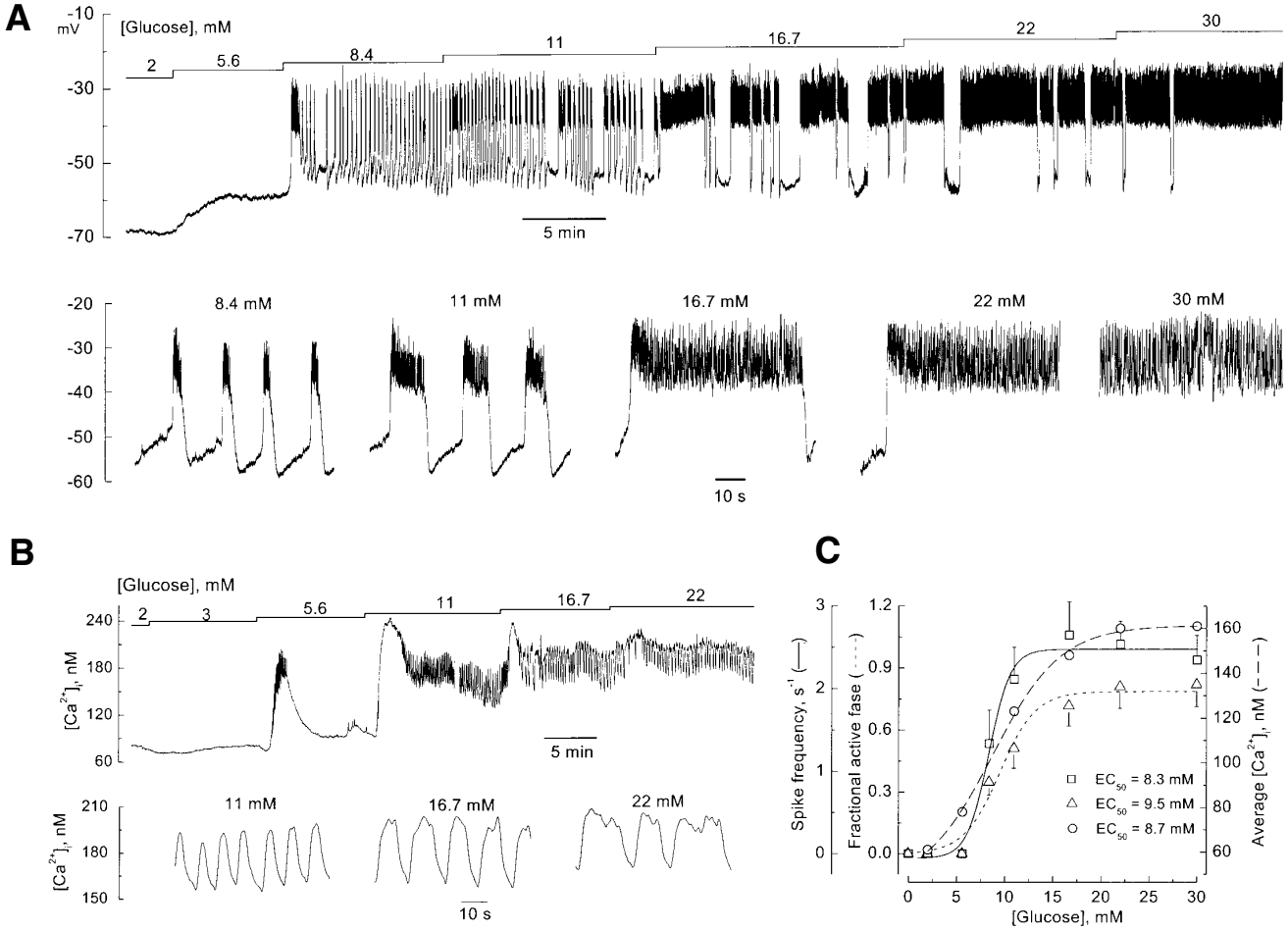

FIG. 6. Dose-dependent effects of glucose stimulation on membrane potential and $[Ca^{2+}]_i$ in mouse islets. Islets were stimulated with increasing glucose concentrations as indicated by the horizontal bars. *A*: Effect on membrane potential (freshly isolated islet). *B*: Effect on $[Ca^{2+}]_i$ (cultured islet). Sample records at each glucose concentration (last 50–70 s) are shown beneath the main traces on an expanded time scale (*A* and *B*). *C*: Effect of increasing glucose concentrations on fractional active-phase duration (percentage of time spent at the depolarized plateau phase), average spike frequency, and average $[Ca^{2+}]_i$, measured at the steady state for each concentration (last 120 s). Data were pooled from the experiments depicted in *A* and *B* and other similar experiments using both freshly isolated and cultured islets (n = 4 and 2 islets for the membrane potential and $[Ca^{2+}]_i$ experiments, respectively). Where available, vertical bars represent mean values ± SE.

is also apparent at each step, especially for intermediate glucose concentrations (e.g., 0.9, 1.2, and 1.6 s^{-1} for 5.6, 8.4, and 11 mmol/l, respectively, in the experiment depicted in Fig. 5*A*). The membrane potential at the foot of the spikes, measured at the steady state for each glucose concentration, was pooled across several experiments and plotted in Fig. 5*C*. This analysis yielded an average EC_{50} for glucose-induced depolarization of the β-cell membrane of 5.9 mmol/l (average membrane potential at saturating glucose –33 ± 3 mV, n = 7 islets).

The effect of glucose on membrane potential of rat β-cells was matched by appreciable $[Ca^{2+}]_i$ increases at all glucose concentrations, starting with 5.6 mmol/l (Fig. 5*B*). The average $[Ca^{2+}]_i$ at the steady state for each glucose concentration was measured from different islets and plotted in Fig. 5*C*, yielding an EC_{50} of 6.9 mmol/l.

Figure 6*A* depicts the typical effect of raising glucose concentration on membrane potential of β-cells from mouse islets. In sharp contrast to rat, mouse β-cells exhibited a pattern of bursting electrical activity at all glucose concentrations in the range 8.4–22 mmol/l. Similar to microdissected mouse islets (22), raising the sugar concentration in this range evoked a dose-dependent increase in fractional active-phase duration (Fig. 6*C*). As a consequence, there was a dose-dependent increase in average spike frequency. The EC_{50} values, calculated from these plots, were 9.5 and 8.3 mmol/l, respectively. Importantly, there were no consistent drifts in either plateau or silent-phase potential as the glucose concentration was raised (average plateau potential in 8.4, 16.7, and 22 mmol/l glucose –38 ± 2, –38 ± 1, and –38 ± 1 mV, respectively; n = 3 islets). It is also worth noting that 5.6 mmol/l glucose depolarized the β-cell membrane by 10 mV without evoking sustained electrical activity.

Fig. 6*B* shows that, in mouse islets, glucose evoked $[Ca^{2+}]_i$ oscillations throughout the intermediate-to-high concentration range (11–22 mmol/l). Moreover, glucose increased the duration of these oscillations in a dose-dependent fashion (3.7 ± 0.1, 9 ± 1, and 11 ± 1 s at 11, 16.7, and 22 mmol/l glucose, respectively; n = 11–23 oscillations for each concentration). There was, however, no consistent change in either peak $[Ca^{2+}]_i$ or the $[Ca^{2+}]_i$ at the trough of the oscillations. We have estimated mean $[Ca^{2+}]_i$ by averaging out the $[Ca^{2+}]_i$ through-

out the last 120-s period at each glucose concentration. The EC_{50} value, estimated from a plot of average $[Ca^{2+}]_i$ versus glucose concentration, was 8.7 mmol/l (Fig. 6*C*).

Effect of glucose on β-cell input resistance. We injected rectangular pulses of hyperpolarizing current (0.1 nA) to assess the effect of glucose stimulation on input resistance to the rat β-cell membrane (Fig. 2*B*). Input resistance was ~108 MΩ at 2 mmol/l glucose, and it increased by 90 and 190% when the cells were stimulated with 5.6 and 16.7 mmol/l glucose, respectively (Fig. 2*C*). These values compare well with the respective values for mouse β-cells (23).

DISCUSSION

Using an improved intracellular recording technique, we have shown that β-cells from rat islets of Langerhans have stable negative membrane potential levels at substimulatory glucose concentrations and that they become depolarized for glucose loads higher than 5.6 mmol/l. Furthermore, glucose-induced depolarization is accompanied by a pronounced rise in cell-input resistance and is antagonized by the K_{ATP} channel activator diazoxide. This is consistent with K_{ATP} channels being inhibited by glucose metabolism, an essential characteristic of the glucose-response–coupling mechanism that has been proposed for pancreatic β-cells of different animal species (24). We have also shown that membrane depolarization in rat β-cells is often accompanied by the firing of action potentials, albeit with an intensity and pattern that are clearly dependent on the extent of depolarization. Specifically, spiking activity is often negligible for membrane potential values more negative than –40 mV. This is consistent with membrane depolarization activating high-threshold voltage-sensitive Ca^{2+} channels, most likely of the L-type, because glucose-induced electrical activity is impaired by the dihydropyridine nifedipine. Massive Ca^{2+} influx associated with the activation of these channels likely accounts for the pronounced $[Ca^{2+}]_i$ changes displayed by rat islets.

The pattern of glucose-induced electrical activity recorded from rat islet β-cells differs from that of mouse β-cells in a number of important points. Whereas the latter exhibit a typical bursting pattern over an extended glucose concentration range (8.4–22.0 mmol/l) (as found in this work and in the study by Atwater et al. [23]), rat β-cells fire action potentials from a nonoscillating membrane potential, regardless of the sugar concentration. This is also evident from the standpoint of $[Ca^{2+}]_i$, which is oscillatory in mouse and nonoscillatory in rat islets. Therefore, it should be emphasized that, in mouse β-cells, glucose increases the duration of the slow membrane potential waves underlying bursting electrical activity without affecting plateau potential and, hence, the characteristics of the action potentials (23); as a result, there is a dose-dependent increase in the duration (not the amplitude) of the associated $[Ca^{2+}]_i$ oscillations. In rat β-cells, in contrast, glucose depolarizes the membrane at the foot of the spikes in a dose-dependent way and more than likely increases the opening probability of the noninactivating fraction of voltage-sensitive Ca^{2+} channels. This action probably explains why the signaling mechanism in rat islets involves changes in the amplitude of the $[Ca^{2+}]_i$ signals.

Different groups have reported varying patterns of $[Ca^{2+}]_i$ and insulin responses of rat islets to glucose stimulation. Using single collagenase-isolated islets, Martin et al. (25) reported the absence of a $[Ca^{2+}]_i$ oscillatory pattern in 95% of the islets stimulated with 11–16.7 mmol/l glucose, whereas Longo et al. (26) and Bergsten et al. (27,28) presented evidence for sustained $[Ca^{2+}]_i$ and insulin oscillations, respectively, in the presence of 10–11 mmol/l glucose. In vitro multi-islet preparations have also been shown to undergo sustained insulin pulsatility in response to 5.5–16.7 mmol/l glucose, albeit with a marked reduction in frequency compared with pulsatile insulin release from single islets (26,29,30). The reason for these apparent discrepancies is not known but could be related to specificities in islet handling (e.g., fresh versus cultured islets, glucose concentration in the culture/preincubation medium and composition of the perifusion solutions). However, it is worth noting that we did not find major differences between fresh and cultured islets in this study. The situation in mouse islets appears to resemble that of human and pig islets, which have been consistently shown to oscillate in response to 11–16.7 mmol/l glucose (31–33). Other parameters of β-cell function have been reported to exhibit marked interspecies differences. For instance, dog and rodent β-cells fire Na^+- and Ca^{2+}-dependent action potentials, respectively, whereas human β-cells display patterns of electrical activity with varying contributions from voltage-sensitive Na^+ and Ca^{2+} channels (18,34,35).

Recent patch-clamp studies of β-cells in intact mouse islets (36) have revealed the presence of a small voltage-activated K^+ conductance, reminiscent of the glucose-activated outward K^+ current described by Rojas et al. (37). This current is strictly dependent on stimulation of Ca^{2+} influx, develops slowly in response to depolarizing pulses, and has the required size to counteract the depolarizing effect of K_{ATP} channel inhibition by glucose. It may therefore represent the primary mechanism by which the burst plateau potential is set at a rather constant level (approximately –35 mV), irrespective of the sugar concentration. In isolated rat β-cells, in turn, glucose failed to stimulate net outward current (37), suggesting that either the cells lack the putative Ca^{2+}-activated K^+ channels or that the size of the Ca^{2+} currents is insufficient to activate these channels to the extent required to regulate the membrane potential. Thus, lack of this compensatory mechanism in rat islet β-cells may explain the fact that glucose depolarizes the cells in a dose-dependent fashion. It should be noted, however, that we cannot rule out the possibility that alternative ionic mechanisms might play a role in this depolarization. For example, Na^+/Ca^{2+} exchange activity has been recently reported to be ~50% higher in rat β-cells (38,39). When operating in the forward mode, this system exchanges three Na^+ ions for one Ca^{2+}, thus providing the net transfer to the cytoplasm of one positive charge per cycle (40). This would cause rat β-cells to be somewhat more depolarized than mouse β-cells, in agreement with the results from our study.

There is no appreciable difference between mouse and rat β-cells with respect to the amplitude of the action potentials, provided that care is taken to match the membrane potential at the foot of the spikes. There is, however, a marked difference concerning the respective rates of depolarization and repolarization: spikes are clearly slower in rat, as evidenced by comparing its first derivatives. It has been proposed that the maximal inward and outward currents can be roughly estimated from the maximal derivatives of the ascending and descending phases of the action potentials, respectively (23). Therefore, we hypothesize that the size of the Ca^{2+} currents responsible for the depolarizing phase of the action potentials

is generally diminished in rat compared with mouse β-cells. Reduced Ca^{2+} loads arising from the activation of voltage-sensitive Ca^{2+} channels may in turn lower the repolarization rate of the action potentials in rat β-cells, assuming that this is partially controlled by Ca^{2+}-activated K^+ channels.

Yet another difference is that average resting membrane potential in rat islet β-cells (2 mmol/l glucose) is 7–10 mV more positive than in mouse β-cells. Two hypotheses may be put forward to explain this difference: mouse β-cells have a larger resting K^+ conductance (higher density of K_{ATP} channels or reduced fraction of K_{ATP} channels inhibited by 2 mmol/l glucose); alternatively, rat β-cells may have a larger resting Na^+ conductance. In a recent patch-clamp study (perforated whole-cell recording configuration, 10 mV pulses), Gopel et al. (41) reported K_{ATP} channel currents of ~26 pA for mouse β-cells in the absence of glucose. Taking into account cell capacitance, this corresponds to a K_{ATP} channel density of ~4 pA/pF. In a similar study conducted using rat β-cells, Hughes et al. (42) reported K_{ATP} channel densities of 4.6 pA/pF. This suggests that K_{ATP} channel density is not significantly different between the two species and is therefore in agreement with our finding that diazoxide brings the resting membrane potential of rat β-cells to a level close to that of mouse β-cells.

We have recalculated available patch-clamp data (43) to assess the dependence of K_{ATP} channel activity on free ATP levels in excised inside-out patches of mouse β-cell membranes. This analysis yielded an IC_{50} for K_{ATP} channel inhibition of 1.4 μmol/l, a value close to that determined by Ashcroft and Kakei (44) for rat β-cells (2 μmol/l). It is likely, then, that the difference between mouse and rat β-cells might be explained by different cytosolic ATP/ADP ratios rather than by a different sensitivity to intracellular ATP. Available measurements of cytosolic intracellular purine nucleotides do not accurately reflect the cytosolic pool, implying that cytosolic ATP/ADP ratios cannot be readily estimated in β-cells. However, it is worth noting that raising the glucose concentration from 0 to 3 mmol/l increased the ATP/ADP ratio (calculated from total ATP and ADP levels) by 10 and 70% in mouse and rat islets, respectively (45–48). This finding reinforces the view that, in rat β-cells exposed to a subthreshold glucose concentration, a higher proportion of K_{ATP} channels is inhibited by a higher ATP/ADP ratio.

We have determined the dose dependency of rat and mouse β-cell function, using a number of electrophysiological and $[Ca^{2+}]_i$ parameters. The estimated EC_{50} values for these parameters lay in the range 5.9–6.9 and 8.3–9.5 mmol/l, respectively, indicating that the dose-response curves for rat β-cells are shifted toward lower glucose concentrations compared with mouse β-cells. This is in keeping with published data for glucose-induced insulin secretion (20,21) and may relate to the fact that low-K_M hexokinase activity accounts for a higher fraction of total glucose phosphorylating activity in rat compared with mouse β-cells (49,50). The differential responses to the lower depolarizing glucose concentration used in our study (5.6 mmol/l) are particularly noteworthy: rat β-cells display a sustained spiking activity, whereas mouse β-cells do not. This is consistent with rat islets having a lower threshold for glucose-induced insulin release.

In summary, our study shows that there are important differences between β-cells from rat and mouse islets, the two most widely used preparations in β-cell research, with respect to early steps in the stimulus-secretion coupling cascade. In particular, rat β-cells lack the compensatory mechanism responsible for generating membrane potential oscillations and for holding the depolarized plateau potential in mouse β-cells. This implies that, contrary to current views, rat islets or β-cells cannot be assumed to bear the electrophysiological properties of mouse islets or β-cells. Realizing the differences between β-cells from both species may lead to the development of new working models of pancreatic β-cell function.

ACKNOWLEDGMENTS

C.M.A. and A.P.S. were supported by the Praxis XXI Program (Portugal). This study was supported in part by Fundação para a Ciência e Tecnologia, Praxis XXI, and the Islet Research European Network Concerted Action of the Commission of the European Communities.

We gratefully acknowledge the School of Medicine at the University of Coimbra for providing the facilities, which were essential for conducting this work.

REFERENCES

1. Bliss CR, Sharp GWG: Glucose-induced insulin release in islets of young rats: time-dependent potentiation and effects of 2-bromostearate. *Am J Physiol* 263:E890–E896, 1992
2. Wollheim CB, Lang J, Regazzi R: The exocytotic process of insulin secretion and its regulation by Ca^{2+} and G-proteins. *Diabetes Rev* 4:276–297, 1996
3. Lenzen S: Insulin secretion by isolated perfused rat and mouse pancreas. *Am J Physiol* 236:E391–E400, 1979
4. Ma YH, Wang J, Rodd GG, Bolaffi JL, Grodsky GM: Differences in insulin secretion between the rat and mouse: role of cAMP. *Eur J Endocrinol* 132:370–376, 1995
5. Zawalich WS, Zawalich KC: Regulation of insulin secretion by phospholipase C. *Am J Physiol* 271:E409–E416, 1996
6. Grill V, Rundfeldt M: Effects of priming with D-glucose on insulin secretion from rat pancreatic islets: increased responsiveness to other secretagogues. *Endocrinology* 105:980–987, 1979
7. Berglund O: Lack of glucose-induced priming of insulin release in the perfused mouse pancreas. *J Endocrinol* 114:185–189, 1987
8. Ikeuchi M, Fujimoto WY, Cook DL: Rat islet cells have glucose-dependent periodic electrical activity. *Horm Metab Res* 16:125–127, 1984
9. Atwater I, Dawson CM, Scott A, Eddlestone G, Rojas E: The nature of the oscillatory behaviour in electrical activity from pancreatic β-cell. *Horm Metab Res* (Suppl. 1) 10:100–107, 1980
10. Santos RM, Rosario LM, Nadal A, Garcia Sancho J, Soria B, Valdeolmillos M: Widespread synchronous $[Ca^{2+}]_i$ oscillations due to bursting electrical activity in single pancreatic islets. *Pflugers Arch* 418:417–422, 1991
11. Silva AM, Rosario LM, Santos RM: Background Ca^{2+} influx mediated by a dihydropyridine- and voltage-insensitive channel in pancreatic β-cells: modulation by Ni^{2+}, diphenylamine-2-carboxylate, and glucose metabolism. *J Biol Chem* 269:17095–17103, 1994
12. Salgado A, Silva AM, Santos RM, Rosario LM: Multiphasic action of glucose and α-ketoisocaproic acid on the cytosolic pH of pancreatic β-cells: evidence for an acidification pathway linked to the stimulation of Ca^{2+} influx. *J Biol Chem* 271:8738–8746, 1996
13. Rosario LM, Barbosa RM, Antunes CM, Silva AM, Abrunhosa AJ, Santos RM: Bursting electrical activity in pancreatic β-cells: evidence that the channel underlying the burst is sensitive to Ca^{2+} influx through L-type Ca^{2+} channels. *Pflugers Arch* 424:439–447, 1993
14. Atwater I, Dawson CM, Eddlestone GT, Rojas E: Voltage noise measurements across the pancreatic β-cell membrane: calcium channel characteristics. *J Physiol (Lond)* 314:195–212, 1981
15. Grynkiewicz G, Poenie M, Tsien RY: A new generation of Ca^{2+} indicators with greatly improved fluorescence properties. *J Biol Chem* 260:3440–3450, 1985
16. Trube G, Rorsman P, Ohno Shosaku T: Opposite effects of tolbutamide and diazoxide on the ATP- dependent K^+ channel in mouse pancreatic β-cells. *Pflugers Arch* 407:493–499, 1986
17. Henquin JC, Meissner HP: Significance of ionic fluxes and changes in membrane potential for stimulus-secretion coupling in pancreatic β-cells. *Experientia* 40:1043–1052, 1984
18. Barnett DW, Pressel DM, Misler S: Voltage-dependent Na^+ and Ca^{2+} currents in human pancreatic islet β-cells: evidence for roles in the generation of action potentials and insulin secretion. *Pflugers Arch* 431:272–282, 1995

19. Curry DL, Bennett LL, Grodsky GM: Dynamics of insulin secretion by the perfused rat pancreas. *Endocrinology* 83:572–584, 1968
20. Henquin JC: D-Glucose inhibits potassium efflux from pancreatic islet cells. *Nature* 271:271–273, 1978
21. Gao ZY, Drews G, Nenquin M, Plant TD, Henquin JC: Mechanisms of the stimulation of insulin release by arginine-vasopressin in normal mouse islets. *J Biol Chem* 265:15724–15730, 1990
22. Rosario LM, Atwater I, Rojas E: Membrane potential measurements in islets of Langerhans from *ob/ob* obese mice suggest an alteration in $[Ca^{2+}]_i$-activated K^+ permeability. *Q J Exp Physiol* 70:137–150, 1985
23. Atwater I, Carroll P, Li MX: Electrophysiology of the pancreatic B-cell. In *Molecular and Cellular Biology of Diabetes Mellitus. I. Insulin Secretion.* Draznin B, Melmed S, Le Roith D, Eds. New York, Alan R. Liss, 1989, p. 49–68
24. Rorsman P, Trube G: Glucose dependent K^+-channels in pancreatic β-cells are regulated by intracellular ATP. *Pflugers Arch* 405:305–309, 1985
25. Martin F, Reig JA, Soria B: Secretagogue-induced $[Ca^{2+}]_i$ changes in single rat pancreatic islets and correlation with simultaneously measured insulin release. *J Mol Endocrinol* 15:177–185, 1995
26. Longo EA, Tornheim K, Deeney JT, Varnum BA, Tillotson D, Prentki M, Corkey BE: Oscillations in cytosolic free Ca^{2+}, oxygen consumption, and insulin secretion in glucose-stimulated rat pancreatic islets. *J Biol Chem* 266:9314–9319, 1991
27. Bergsten P, Hellman B: Glucose-induced amplitude regulation of pulsatile insulin secretion from individual pancreatic islets. *Diabetes* 42:670–674, 1993
28. Bergsten P, Hellman B: Glucose-induced cycles of insulin release can be resolved into distinct periods of secretory activity. *Biochem Biophys Res Commun* 192:1182–1188, 1993
29. Bergstrom RW, Fujimoto WY, Teller DC, De Haen C: Oscillatory insulin secretion in perifused isolated rat islets. *Am J Physiol* 257:E479–E485, 1989
30. Chou HF, Ipp E: Pulsatile insulin secretion in isolated rat islets. *Diabetes* 39:112–117, 1990
31. Martin F, Soria B: Glucose-induced $[Ca^{2+}]_i$ oscillations in single human pancreatic islets. *Cell Calcium* 20:409–414, 1996
32. Kindmark H, Kohler M, Arkhammar P, Efendic S, Larsson O, Linder S, Nilsson T, Berggren PO: Oscillations in cytoplasmic free calcium concentration in human pancreatic islets from subjects with normal and impaired glucose tolerance. *Diabetologia* 37:1121–1131, 1994
33. Bertuzzi F, Zacchetti D, Berra C, Socci C, Pozza G, Pontiroli AE, Grohovaz F: Intercellular Ca^{2+} waves sustain coordinate insulin secretion in pig islets of Langerhans. *FEBS Lett* 379:21–25, 1996
34. Pressel DM, Misler S: Role of voltage-dependent ionic currents in coupling glucose stimulation to insulin secretion in canine pancreatic islet β-cells. *J Membr Biol* 124:239–253, 1991
35. Misler S, Barnett DW, Gillis KD, Pressel DM: Electrophysiology of stimulus-secretion coupling in human β-cells. *Diabetes* 41:1221–1228, 1992
36. Göpel SO, Kanno T, Barg S, Eliasson L, Galvanovskis J, Renström E, Rorsman P: Activation of Ca^{2+}-dependent K^+ channels contributes to rhythmic firing of action potentials in mouse pancreatic β-cells. *J Gen Physiol* 114:759–770, 1999
37. Rojas E, Stokes CL, Mears D, Atwater I: Single-microelectrode voltage clamp measurements of pancreatic β-cell membrane ionic currents in situ. *J Membr Biol* 143:65–77, 1995
38. Van Eylen F, Lebeau C, Albuquerque-Silva J, Herchuelz A: Contribution of Na/Ca exchange to Ca^{2+} outflow and entry in the rat pancreatic β-cell: studies with antisense oligonucleotides. *Diabetes* 47:1873–1880, 1998
39. Van Eylen F, Duquesne V, Bollen A, Herchuelz A: Species-specific transcription pattern and activity of Na/Ca exchange isoforms in pancreatic β-cells. *Diabetologia* 41 (Suppl.1):A130, 1998
40. Gall D, Gromada J, Susa I, Rorsman P, Herchuelz A, Bokvist K: Significance of Na/Ca exchange for Ca^{2+} buffering and electrical activity in mouse pancreatic β-cells. *Biophys J* 76:2018–2028, 1999
41. Gopel S, Kanno T, Barg S, Galvanovskis J, Rorsman P: Voltage-gated and resting membrane currents recorded from B-cells in intact mouse pancreatic islets. *J Physiol (Lond)* 521:717–728, 1999
42. Hughes SJ, Faehling M, Thorneley CW, Proks P, Ashcroft FM, Smith PA: Electrophysiological and metabolic characterization of single β-cells and islets from diabetic GK rats. *Diabetes* 47:73–81, 1998
43. Ohno Shosaku T, Zunkler BJ, Trube G: Dual effects of ATP on K^+ currents of mouse pancreatic β-cells. *Pflugers Arch* 408:133–138, 1987
44. Ashcroft FM, Kakei M: ATP-sensitive K^+ channels in rat pancreatic β-cells: modulation by ATP and Mg^{2+} ions. *J Physiol (Lond)* 416:349–367, 1989
45. Malaisse WJ, Hutton JC, Kawazu S, Sener A: The stimulus-secretion coupling of glucose-induced insulin release: metabolic effects of menadione in isolated islets. *Eur J Biochem* 87:121–130, 1978
46. Zhou XJ, Fadda GZ, Perna AF, Massry SG: Phosphate depletion impairs insulin secretion by pancreatic islets. *Kidney Int* 39:120–128, 1991
47. Warnotte C, Gilon P, Nenquin M, Henquin JC: Mechanisms of the stimulation of insulin release by saturated fatty acids: a study of palmitate effects in mouse β-cells. *Diabetes* 43:703–711, 1994
48. Detimary P, Jonas JC, Henquin JC: Possible links between glucose-induced changes in the energy state of pancreatic β-cells and insulin release: unmasking by decreasing a stable pool of adenine nucleotides in mouse islets. *J Clin Invest* 96:1738–1745, 1995
49. Hedeskov CJ, Capito K: The effect of starvation on insulin secretion and glucose metabolism in mouse pancreatic islets. *Biochem J* 140:423–433, 1974
50. Malaisse WJ, Sener A, Levy J: Stimulus-secretion coupling of glucose-induced insulin release: fasting-induced adaptation of key glycolytic enzymes in isolated islets. *J Biol Chem* 251:1731–1737, 1976